# The lissencephaly protein Lis1 is present in motile mammalian cilia and requires outer arm dynein for targeting to *Chlamydomonas* flagella

**Lotte B. Pedersen[1,2,*], Panteleimon Rompolas[3], Søren T. Christensen[1], Joel L. Rosenbaum[2] and Stephen M. King[3,*]**

[1]Department of Molecular Biology, University of Copenhagen, Universitetsparken 13, DK-2100 Copenhagen OE, Denmark
[2]Department of Molecular, Cellular and Developmental Biology, Yale University, New Haven, CT 06520, USA
[3]Department of Molecular, Microbial and Structural Biology, University of Connecticut Health Center, Farmington, CT 06030, USA
*Authors for correspondence (e-mail: LBPedersen@aki.ku.dk; king@neuron.uchc.edu)

*Accepted 8 December 2006*
*Journal of Cell Science 120, 858-867 Published by The Company of Biologists 2007*
*doi:10.1242/jcs.03374*

## Summary

**Lissencephaly is a developmental brain disorder characterized by a smooth cerebral surface, thickened cortex and misplaced neurons. Classical lissencephaly is caused by mutations in *LIS1*, which encodes a WD-repeat protein involved in cytoplasmic dynein regulation, mitosis and nuclear migration. Several proteins required for nuclear migration in *Aspergillus* bind directly to Lis1, including NudC. Mammalian NudC is highly expressed in ciliated epithelia, and localizes to motile cilia in various tissues. Moreover, a NudC ortholog is upregulated upon deflagellation in *Chlamydomonas*. We found that mammalian Lis1 localizes to motile cilia in trachea and oviduct, but is absent from non-motile primary cilia. Furthermore, we cloned a gene encoding a Lis1-like protein (CrLis1) from *Chlamydomonas*. CrLis1 is a ~37 kDa protein that contains seven WD-repeat domains, similar to Lis1 proteins from other organisms. Immunoblotting using an anti-CrLis1 antibody revealed that this protein is present in the flagellum and is depleted from flagella of mutants with defective outer dynein arm assembly, including one strain that lacks only the α heavy chain/light chain 5 thioredoxin complex. Biochemical experiments confirmed that CrLis1 associates with outer dynein arm components and revealed that CrLis1 binds directly to rat NudC. Our results suggest that Lis1 and NudC are present in cilia and flagella and may regulate outer dynein arm activity.**

Key words: *Chlamydomonas*, Cilia, Dynein, Flagella, Lis1, NudC

## Introduction

Lissencephaly is a developmental brain disorder characterized by a smooth cerebral surface, thickened cortex and misplaced neurons (Wynshaw-Boris and Gambello, 2001). Classical or type I lissencephaly is caused by mutations in *LIS1*, which encodes a WD-repeat protein initially identified as one of the three subunits of the brain platelet-activating factor acetyl-hydrolase (PAFAH)-1b complex (Hattori et al., 1994; Reiner et al., 1993). However, it is now clear that this complex plays no significant role in brain development (Koizumi et al., 2003; Yan et al., 2003). The first clue towards elucidating the molecular pathway by which Lis1 functions in brain development was provided by genetic studies in *Aspergillus nidulans*. Mutations of the *Aspergillus* nuclear distribution (*Nud*) genes compromise the migration of nuclei within the growing hypha. NudF, an ortholog of mammalian Lis1 is involved in this pathway (Xiang et al., 1995), as are cytoplasmic dynein heavy chain (NudA) and the NudC protein (Morris, 2000). Furthermore, mutations in *NudA* are able to suppress the *NudF* nuclear migration phenotype (Willins et al., 1997), suggesting that Lis1/NudF functions in the cytoplasmic dynein pathway. In support of this notion, vertebrate Lis1 coimmunoprecipitates with cytoplasmic dynein and dynactin components in brain extracts, and colocalizes with these protein complexes in mouse brain cortex and various cultured cell types (Faulkner et al., 2000; Smith et al., 2000). The interaction between Lis1 and the cytoplasmic dynein heavy chain (HC) is direct and occurs at multiple sites on the HC molecule, including the motor domain and cargo binding regions (Sasaki et al., 2000; Tai et al., 2002), and may directly stimulate the ATPase activity of the motor (Mesngon et al., 2006). In addition to cytoplasmic dynein and dynactin, Lis1 binds to a variety of other proteins, including NudC (see below), which in turn interact with cytoplasmic dynein and dynactin (reviewed by Vallee and Tsai, 2006). Finally, Lis1 has been found to associate with microtubules and affect microtubule dynamics (Sapir et al., 1997), but this finding is somewhat controversial (Faulkner et al., 2000).

Overexpression of Lis1 in cultured vertebrate cells leads to alterations in microtubule organization, mitotic progression, spindle orientation and chromosome attachment (Faulkner et al., 2000; Smith et al., 2000). Furthermore, microinjection of anti-Lis1 antibody into dividing cultured vertebrate cells results in delayed mitotic progression, suggesting a role for Lis1 in cell division (Faulkner et al., 2000). This is supported by the observation that homozygous *Lis1* knockout mice die before birth (Hirotsune et al., 1998), and that individuals suffering from classical lissencephaly are defective in only one *LIS1* allele (Wynshaw-Boris and Gambello, 2001). Consequently, functional studies of Lis1 during brain development in animals have been performed on heterozygotes and/or hypomorphs that contain reduced levels of Lis1 protein

(Gambello et al., 2003; Hirotsune et al., 1998), or by in utero eletroporation of *LIS1* small interference RNA and dominant negative cDNA constructs (Tsai et al., 2005). These studies have indicated that the primary effect of Lis1 depletion is to disrupt division of neural progenitor cells in the developing brain, as well as their migration (Hatten, 2005; Tsai et al., 2005). Consistent with an important function for Lis1 in brain development, this protein is more highly expressed in neurons than in non-neuronal cells (Smith et al., 2000). Nevertheless, there is still Lis1 protein present in cells from non-neuronal tissue such as liver (Smith et al., 2000), indicating that Lis1 may function in non-neuronal cells as well.

In mammals, motile cilia are involved in fluid transport at the embryonic node, and within many organs (e.g. trachea, oviduct, and brain ventricles); in addition, flagella power sperm motility (Ibanez-Tallon et al., 2003). The dynein-based movement of these microtubular organelles is known to be regulated by several distinct signaling mechanisms including cyclic adenosine monophosphate (cAMP), $Ca^{2+}$, phosphorylation and redox poise (for a review, see Sakato and King, 2004). Furthermore, most cells contain a single non-motile primary cilium that lacks dynein arms and is now considered to function as a sensory organelle (for reviews, see Pazour and Witman, 2003; Christensen et al., 2007). Interestingly, the mammalian NudC protein, which binds directly to Lis1 (Morris et al., 1998), is highly expressed in ciliated epithelia, and localizes to motile cilia in various tissues (Gocke et al., 2000). In addition, the genome of *Chlamydomonas reinhardtii* contains a NudC ortholog, which is upregulated upon deflagellation (Stolc et al., 2005), suggesting that *Chlamydomonas* NudC is a flagellar protein (Lefebvre et al., 1980). However, despite the conservation of ciliary localization of NudC in algae and vertebrates, the physiological relevance of these observations is unclear.

We show here that Lis1 localizes to motile cilia in murine trachea and oviduct, but is absent from non-motile primary cilia in the ovary and in cultured growth-arrested fibroblasts. Furthermore, we cloned a gene encoding a Lis1-like protein (CrLis1) from *Chlamydomonas* and demonstrate that this protein is present in the flagellum and depleted from flagella of mutants with defective outer dynein arm (ODA) assembly. Finally, we provide evidence that CrLis1 associates with the ODA in *Chlamydomonas* flagellar extracts, and binds directly to rat NudC. These findings indicate that Lis1 (and NudC) are present in cilia and flagella, suggesting that they may regulate ODA activity.

## Results

### Mammalian Lis1 localizes to motile cilia

The findings that mammalian NudC localizes to motile cilia in various tissues (Gocke et al., 2000) and interacts directly with Lis1 (Morris et al., 1998) led us to investigate whether mammalian Lis1 is present in motile cilia and flagella. First, we performed immunofluorescence microscopy (IFM) analysis of sections from paraffin-embedded mouse trachea, oviduct and ovary using a goat polyclonal antibody (sc-2577) raised against human Lis1. Immunoblot analysis of lysates derived from the same tissues demonstrated that this antibody specifically crossreacts with murine Lis1 in these tissues and does not recognize other components (Fig. 1). The IFM analysis revealed that Lis1 is present in the motile cilia of trachea and oviduct, but is absent from (non-motile) primary cilia of follicular granulosa cells in the ovary (Fig. 2A,B). Further, Lis1 was absent from primary cilia of growth-arrested NIH3T3 fibroblasts, although punctate localization of Lis1 along the cytoplasmic microtubule network could be observed in these cells (Fig. 2C), consistent with a previously published report (Smith et al., 2000). We also performed IFM analysis of isolated ciliated cells from murine tracheae using a different polyclonal Lis1-specific antibody generated in rabbits (ab2607; Fig. 1). This analysis confirmed that Lis1 localizes to motile cilia (Fig. 3) and was present in multiple punctate structures along the ciliary length. Furthermore, Lis1 was also located in punctate structures throughout the cytoplasm and a strong accumulation of signal was consistently observed at the basal body region from which the cilia assemble (Fig. 3). No ciliary signal was observed if the primary antibody was omitted or if an irrelevant rabbit antibody (against the p24 component of dynactin) was used (Fig. 3). These results indicate that Lis1 is present in motile cilia and is associated with a compartment or substructure of these organelles that is absent from non-motile cilia.

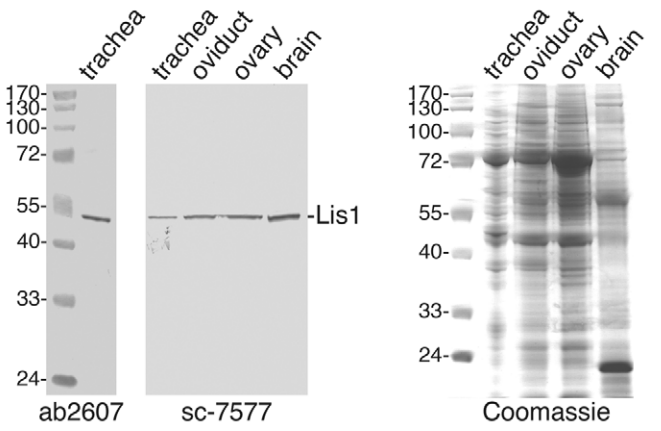


**Fig. 1.** Presence of mammalian Lis1 in trachea, oviduct and ovary. The figure shows the results of an immunoblot analysis of lysates from murine trachea, oviduct and ovary as compared with whole rat brain lysate. Two different polyclonal human Lis1-specific antibodies were used (ab2607 and sc-7577). Note that both antibodies detect a single Lis1 band in the murine lysates that co-migrates with Lis1 from rat brain. The right-hand panel shows a Coomassie-Blue-stained gel run in parallel.

### Identification of a *Chlamydomonas* Lis1 ortholog

To study Lis1 in motile cilia, we used the biflagellate green alga *Chlamydomonas* as a model organism. By BLAST search analysis (Altschul et al., 1990) of the *Chlamydomonas* genome sequence (http://genome.jgi-psf.org/Chlre3/Chlre3.home.html) and EST databases using the human Lis1 polypeptide sequence as query we identified a gene (GenBank accession number DQ647383), hereafter referred to as *CrLIS1*, located on scaffold 20 (JGI version 3, nucleotides 1535128-1537336), which was predicted to encode a 347-residue (37.2 kDa) polypeptide with 45% sequence similarity and 30% identity to human Lis1 (Fig. 4). Southern blot analysis of genomic DNA isolated from *Chlamydomonas* cells demonstrated that there is

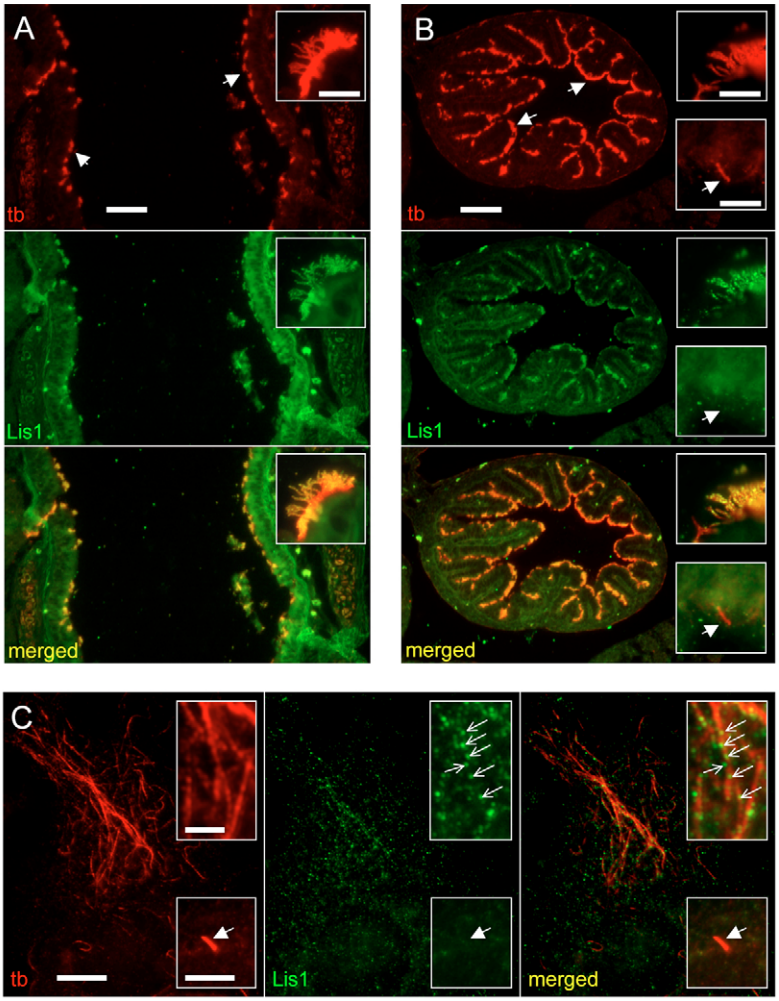


**Fig. 2.** Mammalian Lis1 localizes to motile cilia in tracheae and oviduct. Immunofluorescence microscopy analysis using a goat polyclonal antibody (sc-2577) raised against human Lis1. (A) Tissue section of mouse trachea. Bar, 50 μm. Bar for insets, 10 μm. (B) Tissue section of mouse female reproductive organs. Main image (bar, 50 μm) and upper inset (bar, 10 μm) show motile cilia of the oviduct; lower inset (bar, 10 μm) shows a primary cilium in a follicular granulosa cell in the ovary. (C) Growth-arrested NIH3T3 fibroblast in culture. Main image (bar, 20 μm) and upper inset (bar, 8 μm) show localization of Lis1 along the cytoplasmic network of microtubules (open arrows); lower inset (bar, 20 μm) shows a primary cilium. Bold arrows indicate cilia. tb, acetylated α-tubulin.

a single copy of *CrLIS1* in the *Chlamydomonas* genome (Fig. 5A). Northern blot analysis further revealed that this gene is expressed and is upregulated upon deflagellation in *Chlamydomonas* (Fig. 5B), suggesting that CrLis1 is a flagellar protein (Lefebvre et al., 1980). Analysis of the CrLis1 polypeptide sequence using the SMART algorithm (http://smart.embl-heidelberg.de/) indicated that CrLis1 contains seven WD repeats, similar to Lis1 proteins from other organisms (Reiner and Coquelle, 2005), but lacks the characteristic 33-residue LisH domain at its N-terminus (Fig. 5C). However, ClustalW alignment (Fig. 4) and phylogenetic analysis (Fig. 5D) of multiple WD-repeat proteins indicated that CrLis1 is evolutionarily related to mammalian Lis1.

## CrLis1 is present in flagella

In order to characterize the *CrLIS1* gene product, we cloned the full-length *CrLIS1* open reading frame, expressed it as a fusion protein in *Escherichia coli*, and generated an anti-CrLis1 polyclonal antibody (see Materials and Methods). Immunoblot analysis of isolated flagella using affinity-purified CrLis1 antibody revealed the presence of a ~37 kDa band that co-migrated with recombinant CrLis1 (Fig. 6A). The antibody also crossreacted with a slower migrating band (indicated with an asterisk in Fig. 6A); this band is presumably a component of the axonemal central pair complex as it is missing from flagella of the central pair mutant *pf18* (data not shown). We conclude that the ~37 kDa band detected by the CrLis1 antibody (Fig. 6A) corresponds to CrLis1 and that CrLis1 therefore is present in the flagellum. This conclusion is consistent with the northern blot analysis shown in Fig. 5B.

To determine the localization of CrLis1 within the flagellar compartment, isolated flagella were demembranated with 1% IGEPAL-630 and the resulting axonemes were further extracted with 0.6 M NaCl to remove the dynein arms (King et al., 1986). Immunoblot analysis of these flagellar fractions showed that using this fractionation procedure, CrLis1 is mostly present in the detergent-insoluble axonemal fraction although a small amount of CrLis1 was observed in the detergent-soluble membrane plus matrix fraction as well (Fig. 6B). We note, however, that under different fractionation conditions (e.g. freezing and thawing flagella, adding ATP that can extract axonemal dyneins and/or using alternative detergent types and concentrations) a significant proportion of CrLis1 was present in the soluble membrane plus matrix fraction (Fig. 7 and Fig. 8B).

## CrLis1 is absent from flagella of mutants with defects in ODA assembly

To assess the interactions of CrLis1 within the flagellum, we first screened a variety of mutants with known defects in flagellar assembly and function with respect to the flagellar level of CrLis1. To this end, we isolated flagella from mutant cells and subjected them to sodium dodecyl sulfate-polyacrylamide gel electrophoresis (SDS-PAGE) and immunoblot analysis using the anti-CrLis1 antibody. Interestingly, the results of this analysis revealed that CrLis1 is completely absent from flagella of mutants with defects in ODA assembly (*oda1*, *oda3*, *oda6*), but is present in flagella of mutants lacking other axonemal structures, such as inner dynein arm I1/f (*ida1*), a subset of inner dynein arms I2/3 (*ida4*), radial spokes (*pf14*), and the central pair microtubule complex (*pf18*) (Fig. 6C, and data not shown).

The *Chlamydomonas* ODA contains three distinct HC motor units (α, β and γ) in addition to WD-repeat intermediate chains and multiple LC components, several of which bind directly to the HCs. To further investigate the relationship between CrLis1

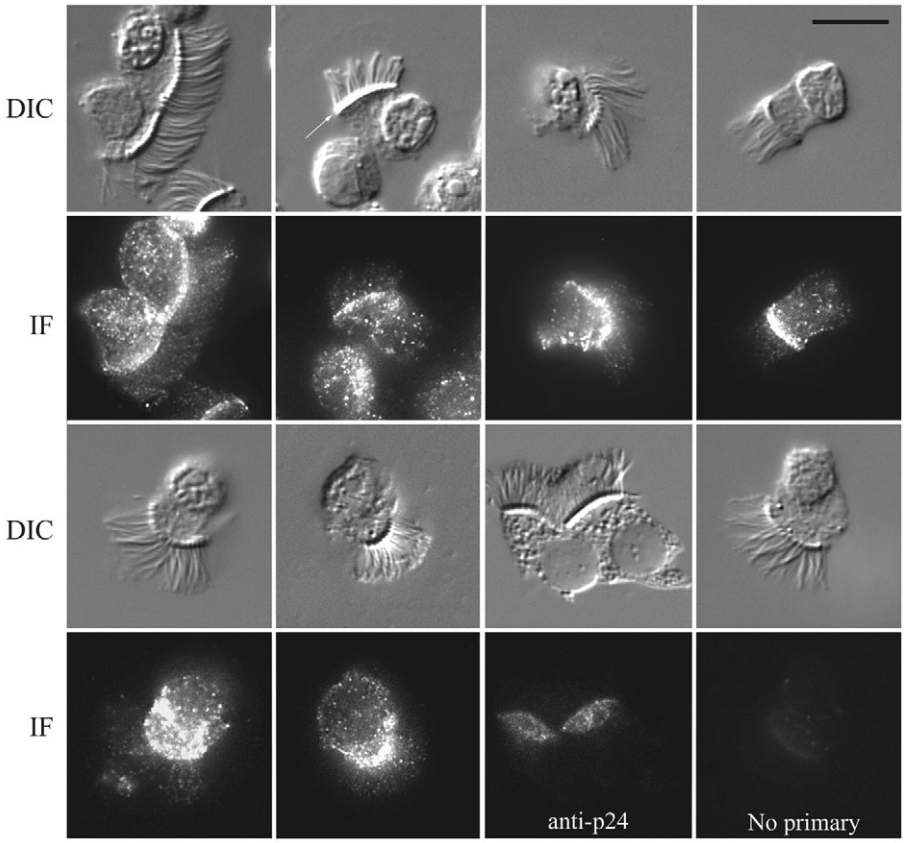


**Fig. 3.** Mammalian Lis1 localizes to motile cilia in isolated airway epithelial cells. Differential interference contrast and corresponding immunofluoresence micrographs of isolated murine tracheal epithelial cells are shown. Except for the two controls at lower right, all micrograph pairs are of cells incubated with a rabbit polyclonal antibody (ab2607) raised against human Lis1. As indicated, the controls were incubated either with no primary antibody or were stained with an irrelevant antibody (against the p24 component of dynactin) to ensure that rabbit immunoglobulin did not bind cilia directly. The prominent structure (white arrow on one panel in top row) underlying the cilia is the layer of basal bodies, which serve as templates for ciliary assembly. Lis1 is present in punctate structures throughout the cytoplasm, shows a strong accumulation in the basal body region and is also clearly present in puncta within cilia. By contrast, no ciliary signal was observed with the dynactin antibody or when the primary antibody was omitted. Bar, 10 μm.

and the ODAs, we next tested for the presence of CrLis1 in mutant flagella lacking specific motor subunits of the ODA complex: the entire outer arm (*oda2*), the outer arm α chain and light chain (LC) 5 thioredoxin (*oda11*), the motor domain of the outer arm β HC (*oda4-s7*), and the *oda4-s7 oda11* double mutant that contains only an intact γ HC (Sakakibara et al., 1991; Sakakibara et al., 1993); for details of ODA structure and organization, see DiBella et al. (DiBella et al., 2004). Immunoblot analysis of these mutant flagella showed that CrLis1 is almost completely missing from *oda2* and *oda11* flagella, but is present in the *oda4-s7* mutant (Fig. 6C). These observations suggest that CrLis1 is associated specifically with the ODA α HC or possibly the LC5 thioredoxin, and that this association is required for targeting to or retention of CrLis1 in the flagellum.

### CrLis1 associates with *Chlamydomonas* ODA and recombinant rat NudC

Our observation that CrLis1 is depleted from flagella of mutants with defects in ODA assembly (Fig. 6C) suggested that CrLis1 might be physically associated with the ODA complex, specifically the ODA α HC or possibly the LC5 thioredoxin, and that this association is essential for CrLis1 flagellar localization. To test whether CrLis1 associates with ODA components, we performed sucrose density gradient centrifugation analysis of 0.6 M NaCl axonemal extracts as well as flagellar membrane plus matrix extract prepared from fresh flagella by extraction with 0.5% Tergitol plus 10 mM ATP (see Materials and Methods), which contains both CrLis1 and ODA components. Individual fractions were probed for CrLis1 as well as IC2 and LC1, which sediment with the ODA αβ and γ HC complexes, respectively (Pfister et al., 1982). This analysis showed that whereas IC2 (a component of the αβ HC subparticle) sedimented at ~20 S and LC1 (part of the γ HC subunit) sedimented at 12 S as expected, CrLis1 was detected only near the top of the gradients with a peak at ~3 S (Fig. 7). This suggests that CrLis1 is not an integral part of the ODA αβ or γ HC complexes and/or that CrLis1 dissociates from these complexes during extraction or sucrose density gradient centrifugation.

Although our sucrose density gradient analysis indicated that CrLis1 is not an integral ODA component, CrLis1 may associate transiently with the ODA αβ HC complex given the results of our ODA mutant analysis (Fig. 6C). To address this issue, we performed a glutathione-S-transferase (GST) pull-down assay. To avoid potential interference of high salt concentration with this assay, we chose to use flagellar membrane plus matrix extracted by freezing and thawing flagella in the presence of 0.05% Nonidet NP-40 and 10 mM ATP rather than using 0.6 M NaCl axonemal extract. The membrane plus matrix detergent and ATP extract was mixed with glutathione beads coated with purified recombinant GST-CrLis1 or GST alone, and bound proteins were collected by centrifugation and analyzed by SDS-PAGE and immunoblotting. The results showed that IC2, which is part of the ODA αβ HC complex (Pfister et al., 1982), cosedimented with GST-CrLis1, but not with GST alone (Fig. 8A,C). Furthermore, α-tubulin did not cosediment with GST-CrLis1 suggesting that association of the outer arm and GST-CrLis1 is specific (Fig. 8A,C).

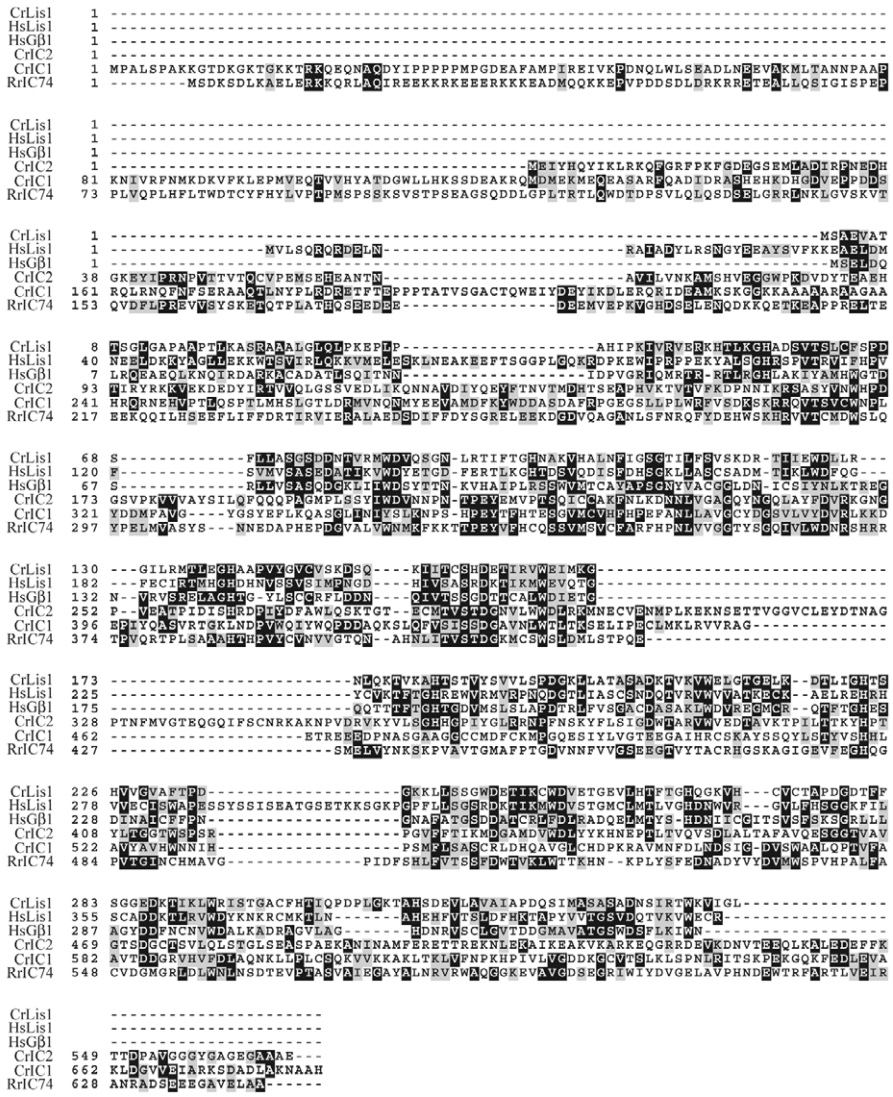


**Fig. 4.** Alignment of CrLis1 with homologous proteins from other organisms. Six WD-repeat proteins were aligned using ClustalW and the output processed with Boxshade. The proteins aligned were *Chlamydomonas* ODA IC1 (CrIC1, Q39578), *Chlamydomonas* ODA IC2 (CrIC2, P27766), rat cytoplasmic dynein IC74 (RrIC74, Q63100), human Gβ1 (HsGβ1, Q5QPR5), human Lis1 (HsLis1, NP000421) and *Chlamydomonas* CrLis1 (CrLis1, DQ647383).

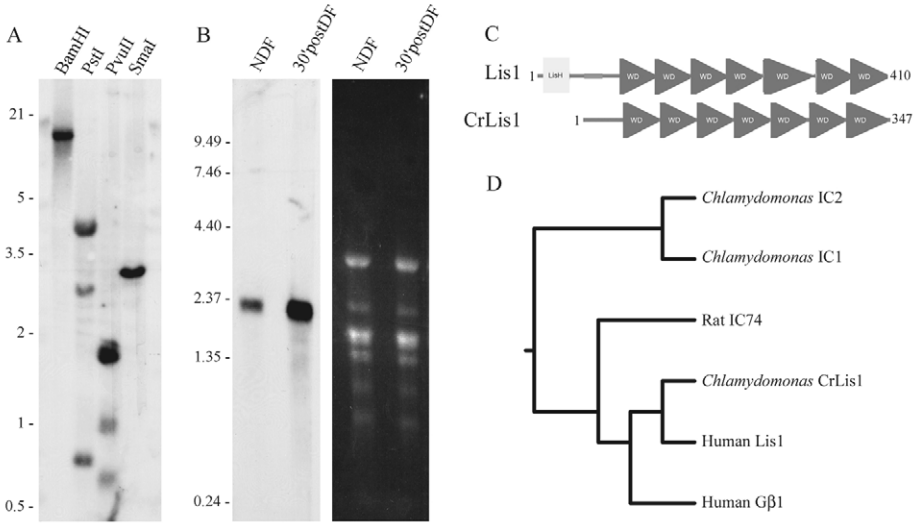


**Fig. 5.** Characterization of the *CrLIS1* gene from *Chlamydomonas*. (A) Southern blot analysis of *Chlamydomonas* genomic DNA using a *CrLIS1*-specific probe. The blot demonstrates that *CrLIS1* is present in a single copy in the *Chlamydomonas* genome. (B) Northern blot analysis of *Chlamydomonas* mRNA showing upregulation of the ~2.2 kb *CrLIS1* mRNA in deflagellated cells (30'postDF) relative to non-deflagellated cells (NDF). (C) SMART analysis (http://smart.embl-heidelberg.de/) of the human Lis1 and CrLis1 polypeptide sequences (see Fig. 4) showing that CrLis1 contains seven WD repeats, as does the human Lis1 protein. However, note the absence of the N-terminal ~30-residue LisH domain in CrLis1. (D) Phylogenetic analysis of CrLis1 based on the ClustalW alignment of WD-repeat proteins (Fig. 4); proteins included in the analysis are *Chlamydomonas* ODA IC1 and IC2, rat cytoplasmic dynein IC74, human Gβ 1, human Lis1 and *Chlamydomonas* CrLis1. CrLis1 is most closely related to mammalian Lis1.

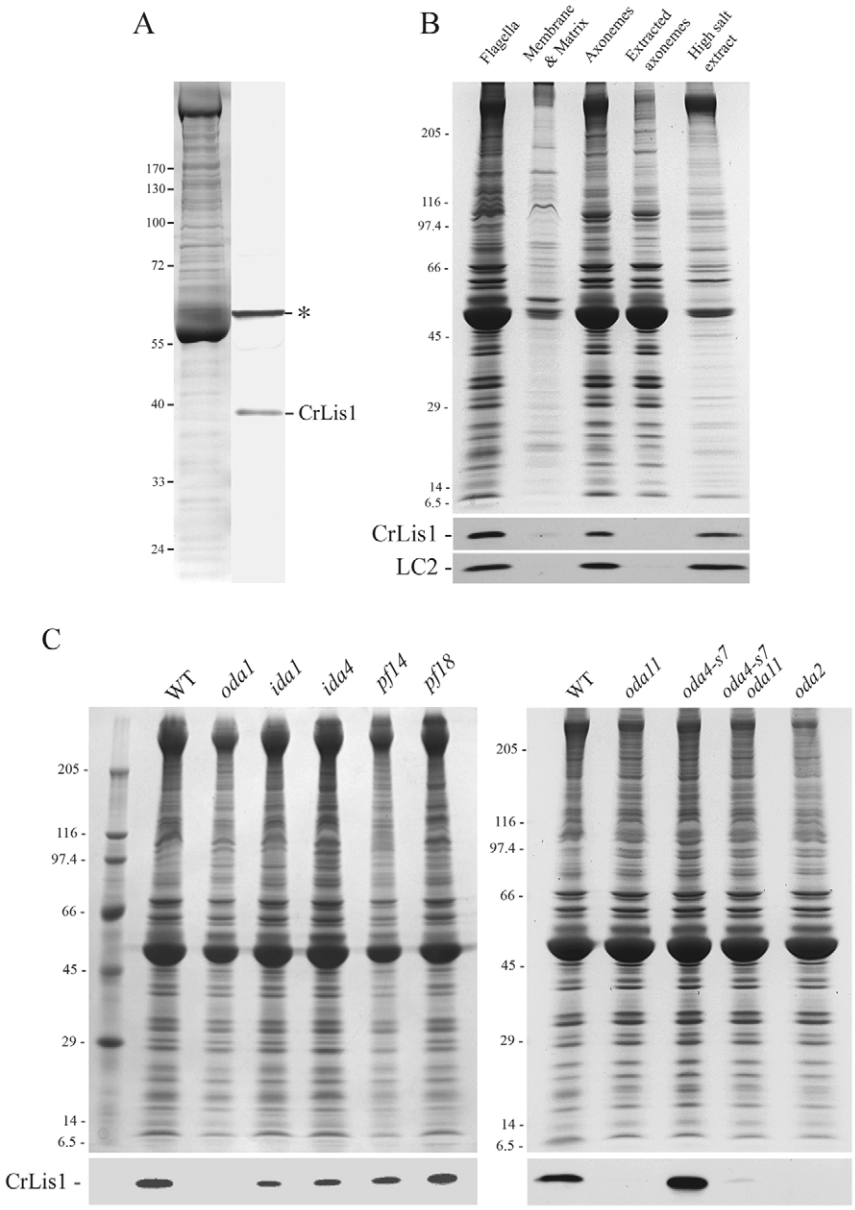


**Fig. 6.** CrLis1 is absent from flagella lacking ODAs. (A) Wild-type flagella were electrophoresed and stained with Coomassie Blue (left panel) or blotted and probed with affinity-purified antibody raised against CrLis1 (right panel). The lower band at ~37 kDa comigrates with recombinant CrLis1 whereas the upper band (marked with an asterisk) is a cross-reacting protein that is completely missing in a mutant that lacks the central pair microtubule complex. (B) Flagella were demembranated with 1% IGEPAL-630 and the resulting axonemes extracted with 0.6 M NaCl. Equivalent amounts of each sample were electrophoresed in a 5-15% acrylamide gradient gel and stained with Coomassie Blue (upper panel) or blotted and probed with antibodies against CrLis1 and LC2 of the ODA (lower panels). Most CrLis1 is associated with axonemes and is extracted by high salt similar to LC2. However, we have observed that under different detergent conditions, more CrLis1 is present in the membrane plus matrix fraction. (C) Flagella from wild-type *Chlamydomonas* and mutants lacking various axonemal substructures were electrophoresed and stained with Coomassie Blue (upper panel) or immunoblotted to detect CrLis1 (lower panel). CrLis1 is specifically missing in strains lacking the ODAs (*oda1* and *oda2*) or only the outer arm α HC and LC5 thiredoxin (*oda11* and *oda4-s7 oda11*).

Given that mammalian Lis1 binds directly to the nuclear movement protein NudC (Morris et al., 1998), and that *Chlamydomonas* contains a *NudC* ortholog (C_590115 in the *Chlamydomonas* genome database) that is upregulated by deflagellation (Stolc et al., 2005), we tested whether rat NudC associates with CrLis1 and the ODA αβ HC complex. For this purpose, flagellar membrane plus matrix detergent and ATP extract (see above) was mixed with glutathione beads coated with purified recombinant GST-rat NudC (GST-rNudC) (Morris et al., 1998) or GST alone, and bound proteins were recovered and analyzed as described above. Interestingly, this analysis showed that CrLis1, IC2 and the α HC-associated LC5 thioredoxin cosedimented with GST-rNudC but not with GST alone (Fig. 8B,C, and data not shown). By contrast, α-tubulin did not cosediment with GST-rNudC, indicating that the association of IC2, LC5 and CrLis1 with GST-rNudC is specific (Fig. 8B,C). Therefore, we conclude that CrLis1 and rNudC interact, at least indirectly, with each other and with the ODA αβ HC complex in *Chlamydomonas* flagella.

## CrLis1 associates directly with rat NudC

Although CrLis1 contains seven WD-repeat domains similar to mammalian Lis1, CrLis1 lacks the N-terminal LisH domain characteristic of other Lis1 proteins (Fig. 5C). Therefore, it was important to determine whether CrLis1 is a functional ortholog of mammalian Lis1 or an unrelated protein with a similar domain structure. Since Lis1 from rat was shown to bind directly to rNudC (Morris et al., 1998), we tested whether CrLis1 similarly could bind directly to rNudC. First, we performed a GST pull-down experiment in which a rat brain extract was mixed with GST-CrLis1 beads and bound proteins were analyzed by SDS-PAGE and immunoblotting using an rNudC-specific antibody (Fig. 8D,E). The results showed that native rNudC specifically interacts, at least indirectly, with GST-CrLis1, but not with GST alone (Fig. 8D,E). Next, we

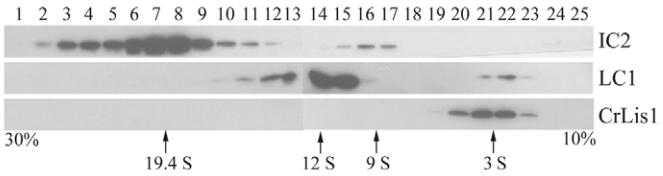


**Fig. 7.** CrLis1 sediments at ~3 S in sucrose density gradients. A Tergitol/ATP extract of *Chlamydomonas* flagella was fractionated in a 10-30% sucrose density gradient. Following electrophoresis, the fractions were probed with antibodies against ODA IC2 and LC1 to locate the ~20 S αβ HC complex and the 12 S γ HC subunit, respectively. Under these conditions, CrLis1 sediments at ~3 S near the top of the gradient. Similar results were obtained when a 0.6 M NaCl axonemal extract was loaded on the gradient.

performed a similar analysis in which purified recombinant maltose-binding protein (MBP; control) or MBP fused in-frame to CrLis1 (MBP-CrLis1) was mixed with beads coated with GST-rNudC, and bound proteins were recovered by centrifugation. SDS-PAGE and immunoblot analysis of the pellet and supernatant fractions demonstrated that MBP-CrLis1 cosedimented with GST-rNudC, whereas MBP alone did not cosediment (Fig. 8F). Since MBP-CrLis1 does not associate with GST alone (Fig. 8G), we conclude that CrLis1 interacts directly with rNudC and hence is a functional ortholog of mammalian Lis1.

## Discussion

In this report, we have demonstrated that the lissencephaly protein Lis1 is specifically present in motile mammalian cilia and furthermore, we have identified a Lis1 homologue in *Chlamydomonas* that depends on the ODA for targeting to and/or retention in the flagellum, and which can bind directly to mammalian NudC.

The *Chlamydomonas* ODA has a molecular mass of ~2 MDa and the isolated particle contains three different HCs (α, β and γ), two distinct ICs, at least ten different LCs and a trimeric docking complex (DiBella and King, 2001; DiBella et al., 2004). Our analysis of various *Chlamydomonas* mutants suggested that CrLis1 is associated specifically with the α HC or the LC5 thioredoxin of the ODA complex. Mammalian Lis1 binds directly to the AAA1 domain and N-terminal stem of cytoplasmic dynein HC (Sasaki et al., 2000; Tai et al., 2002), and biochemical experiments indicated that Lis1 directly stimulates ATP hydrolysis by the motor (Mesngon et al., 2006). Therefore, we predict that CrLis1 associates with the equivalent regions of the ODA α HC, but whether this association affects the ATPase activity of the ODA α HC is uncertain, because CrLis1 lacks the N-terminal LisH domain (Fig. 5C) that is required for Lis1 dimerization and stimulation of cytoplasmic dynein ATPase activity (Mesngon et al., 2006). However, as the *Chlamydomonas* ODA contains three different HC motors whereas cytoplasmic dynein is a HC homodimer, it is possible that this Lis1 dimerization activity is unnecessary

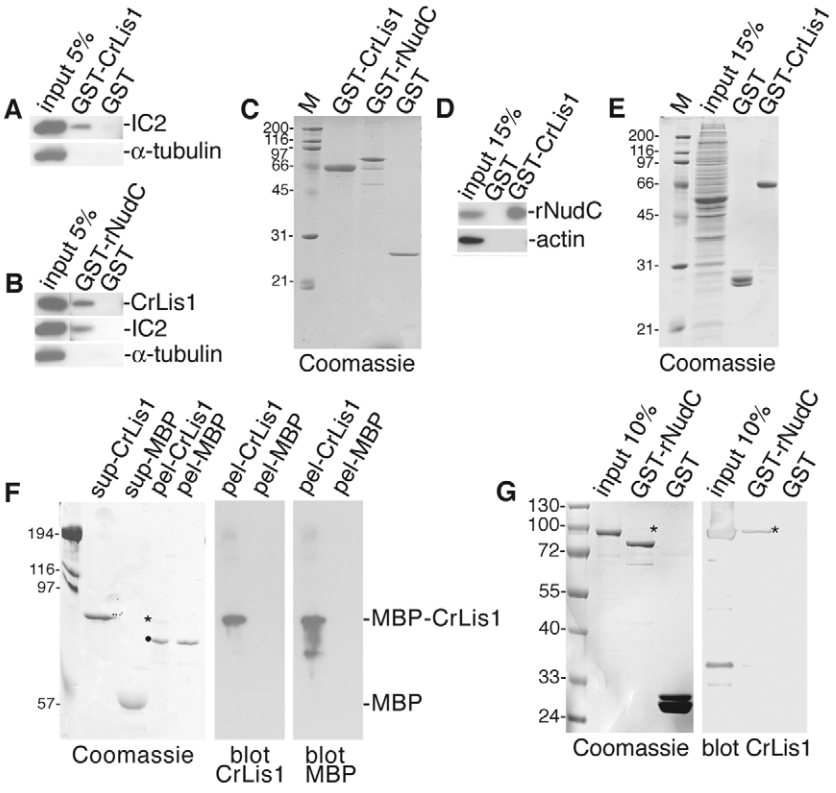


**Fig. 8.** Association of CrLis1 with ODA IC2 and rat NudC. (A) GST pull-down assay of *Chlamydomonas* flagellar membrane plus matrix extract. The extract (input 5%) was mixed with glutathione beads coated with GST-CrLis1 or GST and bound proteins were recovered by centrifugation and analyzed by SDS-PAGE and western blotting using antibodies as indicated. IC2 of the ODA complex cosediments with GST-CrLis1 beads, whereas α-tubulin does not. (B) GST pull-down assay of *Chlamydomonas* flagellar extract showing that CrLis1 and IC2 cosediment with GST-rNudC. (C) Coomassie-Blue-stained gel of the pellet fractions shown in panels A and B. (D,E) GST pull-down assay of rat brain extract (input 15%). Panel D shows a western blot analysis of the input and pellet fractions, panel E shows the corresponding Coomassie-Blue-stained gel. Note that native rNudC cosediments with GST-CrLis1. (F,G) GST pull-down assay showing direct association between CrLis1 and rNudC. In panel F, purified recombinant MBP-CrLis1 (CrLis1) or MBP was mixed with glutathione beads coated with GST-rNudC and bound proteins were recovered by centrifugation. The left-hand panel shows a Coomassie-Blue-stained gel of the pellet (pel) and supernatant (sup) fractions. Note the presence of MBP-CrLis1 (asterisk) in both the supernatant and pellet fractions. The filled circle corresponds to GST-rNudC, which is present in equal amounts in the two pellet lanes. In the middle and right-hand panels, corresponding western blot analyses of the pellet fractions are shown. MBP-CrLis1 cosediments with GST-rNudC whereas MBP does not cosediment. (G) Control experiment in which purified MBP-CrLis1 (input 10%) was mixed with GST-rNudC- or GST-coated beads, subjected to centrifugation and analyzed by SDS-PAGE and immunoblotting. MBP-CrLis1 cosediments with GST-rNudC, but not with GST alone. Asterisks mark the MBP-CrLis1 that is cosedimenting with the GST-rNudC beads.

within the confines of the axonemal superstructure. We note that the α HC exhibits a dominant regulatory effect on the ATP-sensitive microtubule-binding properties of the ODA complex (Sakato and King, 2003), and also that the α HC is phosphorylated in vivo at multiple sites (King and Witman, 1994), indicating that Lis1 potentially could be important for regulation of ODA activity. Such regulation may involve input from a variety of signaling pathways, since *Chlamydomonas* axonemal dyneins are controlled by cAMP, $Ca^{2+}$, redox poise and phosphorylation (Bessen et al., 1980; Howard et al., 1994; Porter and Sale, 2000; Wakabayashi and King, 2006).

Our results indicate that Lis1 (and probably NudC) are associated with the ODA complex of motile cilia and may be involved in regulating its activity. These data do not dispute previous findings demonstrating an essential role for Lis1 in cytoplasmic dynein regulation, mitosis and neuronal migration during embryonic brain development (Faulkner et al., 2000; Gambello et al., 2003; Hirotsune et al., 1998; Smith et al., 2000; Tsai et al., 2005). Rather, we propose that in addition to this function, Lis1 may be involved in regulating ODA activity and ciliary beating in the trachea, oviduct and other ciliated tissues such as the brain ependyma. Interestingly, a recent report demonstrated that beating of brain ependymal cilia is required for normal cerebrospinal fluid (CSF) flow, which in turn is necessary for formation of a concentration gradient of CSF guidance molecules and directional neuronal migration in the adult brain (Sawamoto et al., 2006). Therefore, if Lis1 is required for regulating ODA activity in ependymal cilia, it may be required not only for neuronal migration in the developing embryonic brain, but also in the adult brain.

Typically, genes required for ciliary motility have been associated with a disease known as Kartagener's Syndrome or Primary Ciliary Dyskinesia (PCD) (Afzelius, 1976; Ibanez-Tallon et al., 2003). PCD is characterized by recurrent infections of the upper and lower respiratory tract, male infertility and left-right asymmetry defects or situs inversus. In rare cases, hydrocephalus internus, eye anomalies and cystic kidney disorder are also observed (Ibanez-Tallon et al., 2003). To the best of our knowledge, none of these ciliary diseases have previously been linked to mutations in *LIS1*. However, Lis1 is an essential protein, homozygous *Lis1* knockout mutations in the mouse are embryonic lethal, and individuals suffering from classical lissencephaly contain sporadic mutations in only one *LIS1* allele resulting in Lis1 haploinsufficiency (Hirotsune et al., 1998; Wynshaw-Boris and Gambello, 2001). It is possible that the amount of Lis1 protein produced by these individuals is sufficient for appropriate Lis1 activity in the cilia, but is insufficient to maintain Lis1 cytoplasmic functions. In addition, some types of cilia, such as motile ependymal cilia, are not formed until after birth (Banizs et al., 2005) and hence potential defects in these cilia would not be observed in embryos of homozygous *Lis1* mutant animals, which die between embryonic day 5.5 and 9.5 (Hirotsune et al., 1998). However, in mouse models with one functional *Lis1* gene higher instances of hydrocephalus were reported (Assadi et al., 2003; Hirotsune et al., 1998); a condition that is commonly observed when normal ciliary motility is disrupted (Ibanez-Tallon et al., 2004; Sapiro et al., 2002; Taulman et al., 2001). Consequently, despite the lack of direct genetic and clinical evidence of a cilia-related function for Lis1, it remains likely that Lis1 plays a role in regulating ciliary activity in the brain and other tissues through its association with the ODAs.

## Materials and Methods

### Strains and culture conditions

*C. reinhardtii* strains CC125 MT+ (wild-type), *oda1*, *oda2*, *oda3*, *oda6*, *oda11*, *oda4-s7*, *ida1*, *ida4*, *pf14 and pf18* were obtained from the *Chlamydomonas* Genetics Center (Duke University, Durham, NC). For large-scale flagellar isolation, cells were grown in Tris-acetate-phosphate (TAP) or R medium at 22°C and synchronized with a 14-hour light and 10-hour dark or 15-hour light and 9-hour dark cycle and bubbling with air supplemented with 5% $CO_2$. Cells were collected by centrifugation and resuspended in 10 mM HEPES, pH 7.4, prior to deflagellation.

### PCR, cloning procedures and plasmids

For cloning of *CrLIS1*, the full-length *CrLIS1* cDNA coding region (1041 bp) was PCR-amplified from *C. reinhardtii* wild-type (strain CC125 MT+) cDNA by using the Advantage GC cDNA PCR Kit (BD Biosciences) and primers SAE5′ (5′-GGATCCTCAGCGGAAGTGGCGACCAC-3′) and AVQ3′ (5′-AAGCTTTTGCA CCGCCCTTTCCTTCC-3′). Oligo dT-primed template cDNA was prepared as described previously (Pedersen et al., 2003). The PCR product was ligated into pCR2.1 TOPO (Invitrogen), and the ligated product was then used to transform competent *E. coli* DH5α cells. Plasmids were isolated from the transformants and the inserts from three different plasmids sequenced by standard procedures. The sequences were identical to that derived from alignment of 15 different overlapping ESTs (GenBank accession numbers BG859959.1, BQ824296.1, BI531759.1, BQ820892.1, BG854313.1, BU654540.1, BQ825427.1, BQ809915.1, BU651787.1, BE227932.1, BI717926.1, BQ824140.1, BE452811.1, AW758377.1 and BI530720.1), except that nucleotide 62 was a T instead of C and nucleotide 441 was a T instead of C leading to replacement of alanine at position 21 with valine. These nucleotide changes are probably as a result of strain differences because sequencing of plasmid inserts derived from different PCR reactions gave the same result. The *CrLIS1* open reading frame predicted from the *C. reinhardtii* genome sequence version 3 (http://genome.jgi-psf.org/Chlre3/Chlre3.home.html; scaffold 20 nucleotides 1535128-1537336) lacked the first 147 nucleotides at the 5′ end, but was otherwise identical to that derived from the ESTs. The insert from one of the *CrLIS1*-containing plasmids, named pLP2, was excised with *Bam*H1 and *Hin*dIII, ligated into plasmid pQE30 (Qiagen) and transformed into *E. coli* XL1-Blue cells. One of the transformants (strain LP4) was used for production of 6xHis-tagged CrLis1 fusion protein (see below). The *CrLIS1* coding sequence from strain CC125 MT+ was submitted to GenBank (accession number DQ647383).

For GST-CrLis1 fusion protein, a ~1.1 kb *CrLIS1*-containing fragment was excised from plasmid pLP2 with *Bam*H1 and *Eco*R1 and ligated into plasmid pGEX-2T (Amersham-Pharmacia) to generate an in-frame fusion of GST with the 5′ end of CrLis1. After initial propagation in *E. coli* XL1-Blue cells, the resulting plasmid (pLP21) was transformed into *E. coli* BL21 (DE3) pLysE (Novagen) to generate strain LP22. For generation of rat NudC-GST fusion protein, plasmid pGEX2T containing a ~1.3 kb rat *NUDC* fragment in the *Eco*R1 site (generously provided by Li-Yuan Yu-Lee, Baylor College of Medicine) (Morris et al., 1998) was transformed into *E. coli* BL21 (DE3) pLysE (Novagen) to generate strain LP23. For production of GST, *E. coli* XL1-Blue harboring pGEX5X-2T (Amersham-Pharmacia) without insert (strain LP36) was used.

To generate a MBP-CrLis1 fusion protein, a ~1.1 kb *CrLIS1*-containing fragment was excised from plasmid pLP4 (see above) with *Bam*H1 and *Hin*d111, ligated into plasmid pMalc2 (New England Biolabs) and transformed in *E. coli* XL1-Blue cells. The resulting strain (LP45) was used for production of MBP-CrLis1 fusion protein. For production of MBP, *E. coli* XL1-Blue containing pMALc2 without insert (strain LP44) was used.

### Southern and northern blot analysis

The *CrLIS1* cDNA was used to probe a Southern blot of *Chlamydomonas* genomic DNA restricted with *Bam*HI, *Pst*I, *Pvu*II and *Sma*I, and a northern blot containing total RNA from non-deflagellated cells and from cells that had been allowed to undergo flagellar regeneration for 30 minutes.

### Antibodies

For preparation of anti-CrLis1 antibody, *E. coli* strain LP4 was grown at 37°C in Luria Bertani broth containing 100 μg/ml ampicillin and when the culture had reached an optical density at 600 nm ($OD_{600}$) of 0.5, isopropyl β-D-1-thiogalactopyranoside (IPTG) was added to 1 mM final concentration. After two hours of incubation with IPTG, the cells were harvested by centrifugation and 6xHis-tagged CrLis1 fusion protein was purified under denaturing conditions as recommended by Qiagen (QIAexpressionist, Third Edition, protocols 9 and 14). The purified fusion protein was dialyzed against PBS and used to raise polyclonal antibodies in rabbits at Pocono Rabbit Farm & Laboratory Inc. (Canadensis, PA). The resulting antibody was affinity-purified against the recombinant protein essentially as described previously (Talian et al., 1983). Mouse monoclonal antibodies against α-tubulin, acetylated α-tubulin, and IC2/IC69 of the

*Chlamydomonas* ODA complex (King et al., 1985) were obtained from Sigma. Rabbit polyclonal antibodies against actin and MBP were obtained from Sigma and New England Biolabs, respectively, whereas Li-Yuan Yu-Lee (Baylor College of Medicine) generously provided us with rabbit polyclonal antibody specific for rat NudC (Morris et al., 1998). Rabbit polyclonal antibodies against LC1 and LC2 of the *Chlamydomonas* ODA complex and the p22/24 component of rat dynactin have been described previously (Benashski et al., 1999; Patel-King et al., 1997; Pfister et al., 1998). Antibodies against mammalian Lis1 were obtained from Abcam (ab2607 rabbit polyclonal) and Santa Cruz Biotechnology (sc-2577 goat polyclonal).

### Flagellar isolation and fractionation

Flagella from wild-type and mutant *Chlamydomonas* strains were isolated as described previously (King, 1995; Witman, 1986) and demembranated with 1% IGEPAL-630 (Sigma) in HMEK buffer (10 mM HEPES, 5 mM $MgSO_4$, 25 mM KCl, 0.5 mM EDTA, pH 7.4). The resulting axonemes were then extracted with 0.6 M NaCl to remove the dynein arms (King et al., 1986).

### Sucrose density gradient centrifugation

Sucrose density gradient centrifugation was performed on a 0.6 M NaCl axonemal extract (see above) as well as a flagellar membrane plus matrix extract prepared as follows. Freshly prepared wild-type flagella (Cole et al., 1998) were extracted with HMDEK buffer [10 mM HEPES, 5 mM $MgSO_4$, 25 mM KCl, 0.5 mM EDTA, 1 mM dithiothreitol (DTT), pH 7.2] containing 0.5% Tergitol type NP-40 (Sigma) and 10 mM ATP, and the detergent-insoluble axonemal fraction was removed by centrifugation for 10 minutes at 14,000 ***g***. The rationale for using Tergitol type NP-40 for extraction was that Tergitol appears to be a more gentle detergent than, for example, Nonidet type NP-40 (Wirschell et al., 2004), and we therefore reasoned that Tergitol is less likely to disrupt protein-protein interactions than other detergent types. Flagellar extracts (0.5 ml) were loaded onto 10-30% sucrose density gradients (12.4 ml) prepared in HMDEK buffer, and subjected to centrifugation at 36,000 ***g*** for 18 hours at 4°C. Fractions (0.5 ml each) were collected and analyzed by SDS-PAGE and western blotting. For calibration, a similar gradient was loaded with catalase (232 kDa; 11.3 S), aldolase (158 kDa; 4.4 S) and BSA (67 kDa, 4.4 S) and run in parallel. The sedimentation standards were all obtained from Amersham-Pharmacia. As internal standards, we used IC2 and LC1, which peak at around 19.4 S and 12 S, respectively (Pfister et al., 1982).

### GST pull-down assays

For GST pull-down assays, wild-type (CC125 MT+) *Chlamydomonas* flagella were prepared and stored at –80°C as described previously (Cole et al., 1998). Frozen flagella in HMDEK buffer were thawed, extracted with 0.05% Nonidet type NP-40 (Calbiochem) plus 10 mM ATP, and axonemes removed by two periods of centrifugation at 14,000 ***g*** for 5 minutes. Extract from freshly excised 10-week-old female rat brain frontal cortex (generously supplied by David Wells, MCDB Department, Yale University) was prepared in HMDEK buffer plus 0.05% Nonidet NP-40 using a Dounce homogenizer, and the extract was cleared by centrifugation at 14,000 ***g*** for 10 minutes.

GST fusion proteins were produced by growing *E. coli* strains LP22 (GST-CrLis1), LP23 (GST-rat NudC) or LP36 (GST) at 30°C in Luria Bertani broth supplemented with appropriate antibiotics until the cultures had reached an $OD_{600}$ of 0.5. IPTG was then added to 1 mM final concentration and the cultures were incubated overnight at 18°C, harvested by centrifugation, rinsed in PBS and flash-frozen in liquid $N_2$. Frozen cells from 500 ml of culture were lysed by incubation in 50 ml PBS plus 0.1% Nonidet NP-40 for 10 minutes at room temperature, the DNA sheared by sonication, and the lysates cleared by two periods of centrifugation at 12,000 ***g*** for 10 minutes. The cleared lysates were each incubated with 1 ml of glutathione-agarose (Sigma) for 1 hour at 4°C, the agarose beads collected by centrifugation and washed three times for 10 minutes with HMDEK buffer containing 0.1% Nonidet NP-40.

Growth, induction and harvest of bacteria expressing MBP-CrLis1 (LP45) or MBP (LP44) were done as described above for GST fusion proteins, and frozen bacterial pellets were lysed in PBS containing 1 mg/ml of lysozyme and 0.1% Nonidet NP-40. After sonicating the lysates to shear the DNA, followed by centrifugation to pellet cellular debris, the cleared lysates were incubated for 1 hour at 4°C with amylose resin (New England Biolabs). The resin was collected by centrifugation, washed three times for 10 minutes in PBS plus 0.1% Nonidet NP-40, and bound proteins were eluted with PBS plus 10 mM maltose. After concentrating the proteins in Centricon 10 tubes (Millipore), glycerol was added to 25% final volume and the samples stored at –80°C until use.

GST fusion protein-coated beads were incubated with either *Chlamydomonas* flagellar extract (~2-3 mg/ml), rat brain extract (~2-3 mg/ml) or purified MBP-CrLis1 or MBP (0.1 mg/ml) for 1 hour at 4°C, the beads collected by centrifugation and washed three times for 10 minutes with HMDEK buffer plus 0.05% Nonidet NP-40.

### SDS-PAGE and immunoblot analysis

Isolated *Chlamydomonas* flagella, flagellar fractions or pellets from GST pull-down assays were solubilized in Laemmli buffer and analyzed by SDS-PAGE and immunoblotting using standard procedures. Freshly excised murine tracheae, oviduct and ovary as well as whole rat brain were solubilized in PBS containing 1% SDS, vortexed vigorously in the presence of glass beads, and the DNA sheared with a syringe. The lysates were cleared by centrifugation, mixed with Laemmli buffer and analyzed by SDS-PAGE and immunoblotting using standard procedures. Secondary antibodies were detected by chemiluminescence or colorometric methods. For immunoblotting, antibodies were diluted as follows: anti-CrLis1, 1:1000; anti-IC2, 1:4000; anti-α-tubulin, 1:1000; anti-rat NudC, 1:500; anti-actin, 1:1000; anti-LC1, 1:100; anti-LC2, 1:100; anti-MBP, 1:4000; anti-Lis1 ab2607, 1:1000; anti-Lis1 sc-7577, 1:500.

### Immunofluorescence microscopy of paraffin-embedded tissue sections and cultured fibroblasts

Oviduct, ovaries and tracheae were removed from adult female mice, fixed, embedded in paraffin and cut into 8-μm-thick sections that were collected on microscope slides for IFM analysis as previously described (Teilmann and Christensen, 2005). NIH3T3 fibroblasts were cultured for 24 hours in serum-free medium to induce growth arrest, fixed and subjected to IFM analysis as described by Schneider et al. (Schneider et al., 2005). Fixed cells and tissue sections were incubated at room temperature for 2 hours with mouse monoclonal anti-acetylated α-tubulin antibody (diluted 1:50,000) and goat polyclonal Lis1 antibody (diluted 1:200). After washing, cells and tissue sections were incubated for 1 hour at room temperature with Alexa Fluor 568-conjugated rabbit anti-mouse immunoglobulin G (IgG) and Alexa Fluor 488-conjugated donkey anti-goat IgG secondary antibodies (Molecular Probes). Sections and cells were mounted in PBS containing 70% glycerol and 2% N-propylgallate and the slides sealed with nail polish. Samples were observed on an Eclipse E600 microscope (Nikon) with EPI-FL3 filters and MagnaFire cooled CCD camera (Optronics, Goleta, CA), and digital images were processed using Adobe Photoshop version 6.0.

### Immunofluorescence microscopy of isolated tracheal cells

Adult mice were euthanized by $CO_2$ asphyxiation and their tracheae removed and treated with Hanks' balanced salt solution supplemented with 25 mM HEPES, pH 7.4. Ciliated cells were obtained by scratching the epithelial surface with a scalpel or alternatively by enzymatic digestion with 0.5% type XIV bacterial protease (Sigma). Enzymatically isolated cells were kept in Dulbecco's modified Eagle's medium (DMEM) supplemented with 25 mM HEPES, pH 7.4, 10% fetal bovine serum and checked for viability by assessing ciliary beating. Cells were briefly washed in PBS pH 7.4 and left to adhere on poly-L-lysine-coated slides prior to fixation with 4% paraformadehyde for 15 minutes at room temperature. Cells were permeabilized with 1% IGEPAL CA-630 (Sigma), blocked with 5% normal goat serum and incubated with rabbit polyclonal anti-hLis1 antibody (ab2607, Abcam) or anti-p24 dynactin antibody at 4°C for 16 hours. Subsequently, samples were incubated with Alexa Fluor 488-conjugated goat anti-rabbit IgG (Molecular Probes) and DNA counterstained with DAPI. Cells were observed with an Olympus BX51 epifluorescence microscope equipped with a Magnafire CCD camera for image acquisition.

We thank Ramila Patel-King and Oksana Gorbatyuk (University of Connecticut Health Center) for their assistance with molecular and biochemical analysis of CrLis1, David Wells (Yale University) and Gert Christoffersen (University of Copenhagen) for providing us with rat brain lysates, Li-Yuan Yu-Lee (Baylor College of Medicine) for rat NudC plasmids and antibodies, and Anne Grete Byskov (Rigshospitalet, Copenhagen, Denmark) for supplying us with murine tissue sections for IFM and immunoblot analyses. Hue Tran provided expert technical assistance with *Chlamydomonas* culture and flagellar preparations, and Christian A. Clement assisted with IFM. This work was supported by grants from the National Institutes of Health to J.L.R. and S.M.K., from the Danish Natural Science Research Council (no. 272-05-0411) and the Novo Nordisk Foundation to L.B.P., and from the Carlsberg Foundation to S.T.C. S.M.K. is an investigator of the Patrick and Catherine Weldon Donaghue Medical Research Foundation.

## References

**Afzelius, B. A.** (1976). A human syndrome caused by immotile cilia. *Science* **193**, 317-319.

**Altschul, S. F., Gish, W., Miller, W., Myers, E. W. and Lipman, D. J.** (1990). Basic local alignment search tool. *J. Mol. Biol.* **215**, 403-410.

**Assadi, A. H., Zhang, G., Beffert, U., McNeil, R. S., Renfro, A. L., Niu, S., Quattrocchi, C. C., Antalffy, B. A., Sheldon, M., Armstrong, D. D. et al.** (2003). Interaction of reelin signaling and Lis1 in brain development. *Nat. Genet.* **35**, 270-276.

**Banizs, B., Pike, M. M., Millican, C. L., Ferguson, W. B., Komlosi, P., Sheets, J., Bell, P. D., Schwiebert, E. M. and Yoder, B. K.** (2005). Dysfunctional cilia lead to altered ependyme and choroid plexus function, and result in the formation of hydrocephalus. *Development* **132**, 5329-5339.

**Benashski, S. E., Patel-King, R. S. and King, S. M.** (1999). Light chain 1 from the *Chlamydomonas* outer dynein arm is a leucine-rich repeat protein associated with the motor domain of the γ heavy chain. *Biochemistry* **38**, 7253-7264.

**Bessen, M., Fay, R. B. and Witman, G. B.** (1980). Calcium control of waveform in isolated flagellar axonemes of *Chlamydomonas*. *J. Cell Biol.* **86**, 446-455.

**Christensen, S. T., Pedersen, L. B., Schneider, L. and Satir, P.** (2007). Sensory cilia and integration of signal transduction in human health and disease. *Traffic* **8**, 97-109.

**Cole, D. G., Diener, D. R., Himelblau, A. L., Beech, P. L., Fuster, J. C. and Rosenbaum, J. L.** (1998). *Chlamydomonas* kinesin-II-dependent intraflagellar transport (IFT): IFT particles contain proteins required for ciliary assembly in *Caenorhabditis elegans* sensory neurons. *J. Cell Biol.* **141**, 993-1008.

**DiBella, L. M. and King, S. M.** (2001). Dynein motors of the *Chlamydomonas* flagellum. *Int. Rev. Cytol.* **210**, 227-268.

**DiBella, L. M., Sakato, M., Patel-King, R. S., Pazour, G. J. and King, S. M.** (2004). The LC7 light chains of *Chlamydomonas* flagellar dyneins interact with components required for both motor assembly and regulation. *Mol. Biol. Cell* **15**, 4633-4646.

**Faulkner, N. E., Dujardin, D. L., Tai, C.-Y., Vaughan, K. T., O'Connell, C. B., Wang, Y.-L. and Vallee, R. B.** (2000). A role for the lissencephaly gene *LIS1* in mitosis and cytoplasmic dynein function. *Nat. Cell Biol.* **2**, 784-791.

**Gambello, M., Darling, D. L., Yingling, J., Tanaka, T., Gleeson, J. G. and Wynshaw-Boris, A.** (2003). Multiple dose-dependent effects of *Lis1* on cerebral cortical development. *J. Neurosci.* **23**, 1719-1729.

**Gocke, C. D., Osmani, S. A. and Miller, B. A.** (2000). The human homologue of *Aspergillus* nuclear migration gene *nudC* is preferentially expressed in dividing cells and ciliated epithelia. *Histochem. Cell Biol.* **114**, 293-301.

**Hatten, M. E.** (2005). LIS-less neurons don't even make it to the starting gate. *J. Cell Biol.* **170**, 867-871.

**Hattori, M., Adachi, H., Tsujimoto, M., Arai, H. and Inoue, K.** (1994). Miller-Dieker lissencephaly gene encodes a subunit of brain platelet-activating factor. *Nature* **370**, 216-218.

**Hirotsune, S., Fleck, M. W., Gambello, M. J., Bix, G. J., Chen, A., Clark, G. D., Ledbetter, D. H., McBain, C. J. and Wynshaw-Boris, A.** (1998). Graded reduction of *Pafah1b (Lis1)* activity results in neuronal migration defects and early embryonic lethality. *Nat. Genet.* **19**, 333-339.

**Howard, D. R., Habermacher, G., Glass, D. B., Smith, E. F. and Sale, W. S.** (1994). Regulation of *Chlamydomonas* flagellar dynein by an axonemal protein kinase. *J. Cell Biol.* **127**, 1683-1692.

**Ibanez-Tallon, I., Heintz, N. and Omran, H.** (2003). To beat or not to beat: roles of cilia in development and disease. *Hum. Mol. Genet.* **12**, R27-R35.

**Ibanez-Tallon, I., Pagenstecher, A., Fliegauf, M., Olbrich, H., Kispert, A., Ketelsen, U.-P., North, A., Heintz, N. and Omran, H.** (2004). Dysfunction of axonemal dynein heavy chain Mdnah5 inhibits ependymal flow and reveals a novel mechanism for hydrocephalus formation. *Hum. Mol. Genet.* **13**, 2133-2141.

**King, S. M.** (1995). Large-scale isolation of *Chlamydomonas* flagella. *Methods Cell Biol.* **47**, 9-12.

**King, S. M. and Witman, G. B.** (1994). Multiple sites of phosphorylation within the α heavy chain of *Chlamydomonas* outer arm dynein. *J. Biol. Chem.* **269**, 5452-5457.

**King, S. M., Otter, T. and Witman, G. B.** (1985). Characterization of monoclonal antibodies against *Chlamydomonas* flagellar dyneins by high-resolution protein blotting. *Proc. Natl. Acad. Sci. USA* **82**, 4717-4721.

**King, S. M., Otter, T. and Witman, G. B.** (1986). Purification and characterization of *Chlamydomonas* flagellar dyneins. *Meth. Enzymol.* **134**, 291-306.

**Koizumi, H., Yamaguchi, N., Hattori, M., Ishikawa, T. O., Aoki, J., Taketo, M. M., Inoue, K. and Arai, H.** (2003). Targeted disruption of intracellular type I platelet activating factor-acetylhydrolase catalytic subunits causes severe impairment in spermatogenesis. *J. Biol. Chem.* **278**, 12489-12494.

**Lefebvre, P. A., Silflow, C. D., Wieben, E. D. and Rosenbaum, J. L.** (1980). Increased levels of mRNAs for tubulin and other flagellar proteins after amputation or shortening of *Chlamydomonas* flagella. *Cell* **20**, 469-477.

**Mesngon, M. T., Tarricone, C., Hebbar, S., Guillotte, A. M., Schmitt, E. W., Lanier, L., Musacchio, A., King, S. J. and Smith, D. S.** (2006). Regulation of cytoplasmic dynein ATPase by Lis1. *J. Neurosci.* **26**, 2132-2139.

**Morris, N. R.** (2000). Nuclear migration: from fungi to mammalia brain. *J. Cell Biol.* **148**, 1097-1101.

**Morris, S. M., Albrecht, U., Reiner, O., Eichele, G. and Yu-Lee, L. Y.** (1998). The lissencephaly gene product Lis1, a protein involved in neuronal migration, interacts with a nuclear movement protein NudC. *Curr. Biol.* **8**, 603-606.

**Patel-King, R. S., Benashski, S. E., Harrison, A. and King, S. M.** (1997). A *Chlamydomonas* homologue of the putative murine *t* complex distorter Tctex-2 is an outer arm dynein light chain. *J. Cell Biol.* **137**, 1081-1090.

**Pazour, G. J. and Witman, G. B.** (2003). The vertebrate primary cilium is a sensory organelle. *Curr. Opin. Cell Biol.* **15**, 105-110.

**Pedersen, L. B., Geimer, S., Sloboda, R. D. and Rosenbaum, J. L.** (2003). The microtubule plus end-tracking protein EB1 is localized to the flagellar tip and basal bodies in *Chlamydomonas reinhardtii*. *Curr. Biol.* **13**, 1969-1974.

**Pfister, K. K., Fay, R. B. and Witman, G. B.** (1982). Purification and polypeptide composition of dynein ATPases from *Chlamydomonas* flagella. *Cell Motil.* **2**, 525-547.

**Pfister, K. K., Benashski, S. E., Dillman, J. F., Patel-King, R. S. and King, S. M.** (1998). Identification and molecular characterization of the p24 dynactin light chain. *Cell Motil. Cytoskeleton* **41**, 154-167.

**Porter, M. E. and Sale, W. S.** (2000). The 9+2 axoneme anchors multiple inner arm dyneins and a network of kinases and phosphatases that control motility. *J. Cell Biol.* **151**, F37-F42.

**Reiner, O. and Coquelle, F. M.** (2005). Missense mutations resulting in type 1 lissencephaly. *Cell. Mol. Life Sci.* **62**, 425-434.

**Reiner, O., Carrozzo, R., Shen, Y., Wehnert, M., Faustinella, F., Dobyns, W. B., Caskey, C. T. and Ledbetter, D. H.** (1993). Isolation of a Miller-Dieker lissencephaly gene containing G protein subunit-like repeats. *Nature* **364**, 717-721.

**Sakakibara, H., Mitchell, D. R. and Kamiya, R.** (1991). A *Chlamydomonas* outer arm dynein mutant missing the α heavy chain. *J. Cell Biol.* **113**, 615-622.

**Sakakibara, H., Takada, S., King, S. M., Witman, G. B. and Kamiya, R.** (1993). A *Chlamydomonas* outer arm dynein mutant with a truncated β heavy chain. *J. Cell Biol.* **122**, 653-661.

**Sakato, M. and King, S. M.** (2003). Calcium regulates ATP-sensitive microtubule binding by *Chlamydomonas* outer arm dynein. *J. Biol. Chem.* **278**, 43571-43579.

**Sakato, M. and King, S. M.** (2004). Design and regulation of the $AAA^+$ microtubule motor dynein. *J. Struct. Biol.* **146**, 58-71.

**Sapir, T., Elbaum, M. and Reiner, O.** (1997). Reduction of microtubule catastrophe events by LIS1, platelet-activating factor acetylhydrolase subunit. *EMBO J.* **16**, 6977-6984.

**Sapiro, R., Kostetskii, I., Olds-Clarke, P., Gerton, G. L., Radice, G. L. and Strauss, J. F., III** (2002). Male infertility, impaired sperm motility, and hydrocephalus in mice deficient in sperm-associated antigen 6. *Mol. Cell. Biol.* **22**, 6298-6305.

**Sasaki, S., Shionoya, A., Ishida, M., Gambello, M., Yingling, J., Wynshaw-Boris, A. and Hirotsune, S.** (2000). A LIS1/NUDEL/cytoplasmic dynein heavy chain complex in the developing and adult nervous system. *Neuron* **28**, 681-696.

**Sawamoto, K., Wichterle, H., Gonzales-Perez, O., Cholfin, J. A., Yamada, M., Spassky, N., Murcia, N. S., Garcia-Verdugo, J. M., Marin, O., Rubenstein, J. L. R. et al.** (2006). New neurons follow the flow of cerebrospinal fluid in the adult brain. *Science* **311**, 629-632.

**Schneider, L., Clement, C. A., Teilmann, S. C., Pazour, G. J., Hoffmann, E. K., Satir, P. and Christensen, S. T.** (2005). PDGFRαα signaling is regulated through the primary cilium in fibroblasts. *Curr. Biol.* **15**, 1861-1866.

**Smith, D. S., Niethammer, M., Ayala, R., Zhou, Y., Gambello, M. J., Wynshaw-Boris, A. and Tsai, J. W.** (2000). Regulation of cytoplasmic dynein behaviour and microtubule organization by mammalian Lis1. *Nat. Cell Biol.* **2**, 767-775.

**Stolc, V., Samanta, M. P., Tongprasit, W. and Marshall, W. F.** (2005). Genome-wide transcriptional analysis of flagellar regeneration in *Chlamydomonas*. *Proc. Natl. Acad. Sci. USA* **102**, 3703-3707.

**Tai, C.-Y., Dujardin, D. L., Faulkner, N. E. and Vallee, R. B.** (2002). Role of dynein, dynactin, and CLIP-170 interactions in LIS1 kinetochore function. *J. Cell Biol.* **156**, 959-968.

**Talian, J. C., Olmsted, J. B. and Goldman, R. D.** (1983). A rapid procedure for preparing fluorescein-labeled specific antibodies from whole antiserum: its use in analyzing cytoskeletal architecture. *J. Cell Biol.* **97**, 1277-1282.

**Taulman, P. D., Haycraft, C. J., Balkovetz, D. F. and Yoder, B. K.** (2001). Polaris, a protein involved in left-right axis patterning, localizes to basal bodies and cilia. *Mol. Biol. Cell* **12**, 589-599.

**Teilmann, S. C. and Christensen, S. T.** (2005). Localization of the angiopoeitin receptors Tie-1 and Tie-2 on the primary cilia in the female reproductive organs. *Cell Biol. Int.* **29**, 340-346.

**Tsai, J. W., Chen, Y., Kriegstein, A. R. and Vallee, R. B.** (2005). LIS1 RNA interference blocks neural stem cell division, morphogenesis, and motility. *J. Cell Biol.* **170**, 935-945.

**Vallee, R. B. and Tsai, J. W.** (2006). The cellular roles of the lissencephaly gene LIS1, and what they tell us about brain development. *Genes Dev.* **20**, 1384-1393.

**Wakabayashi, K. and King, S. M.** (2006). Modulation of *Chlamydomonas reinhardtii* flagellar motility by redox poise. *J. Cell Biol.* **173**, 743-754.

**Willins, D. A., Liu, B., Xiang, X. and Morris, N. R.** (1997). Mutations in the heavy chain of cytoplasmic dynein suppress the *nudF* nuclear migration mutation of *Aspergillus nidulans*. *Mol. Gen. Genet.* **255**, 194-200.

**Wirschell, M., Pazour, G., Yoda, A., Hirono, M., Kamiya, R. and Witman, G. B.** (2004). Oda5p, a novel axonemal protein required for assembly of the outer dynein arm and an associated adenylate kinase. *Mol. Biol. Cell* **15**, 2729-2741.

**Witman, G. B.** (1986). Isolation of *Chlamydomonas* flagella and flagellar axonemes. *Meth. Enzymol.* **134**, 280-290.

**Wynshaw-Boris, A. and Gambello, M.** (2001). LIS1 and dynein motor function in neuronal migration and development. *Genes Dev.* **15**, 639-651.

**Xiang, X., Osmani, A. H., Osmani, S. A., Xin, M. and Morris, N. R.** (1995). *NudF*, a nuclear migration gene in *Aspergillus nidulans,* is similar to the human *LIS-1* gene required for neuronal migration. *Mol. Biol. Cell* **6**, 297-310.

**Yan, W., Assadi, A. H., Wynshaw-Boris, A., Eichele, G., Matzuk, M. M. and Clark, G. D.** (2003). Previously uncharacterized roles of platelet-activating factor acetylhydrolase 1b complex in mouse spermatogenesis. *Proc. Natl. Acad. Sci. USA* **100**, 7189-7194.